Cited by SCI

ISSN 0254-5861
CN35-1112/TQ
CODEN JHUADF

CHINESE JOURNAL OF STRUCTURAL CHEMISTRY

结构化学

Sponsored by Chinese Chemical Society
Fujian Institute of Research on the Structure of Matter, The Chinese Academy of Sciences
Co-sponsored by Peiking University

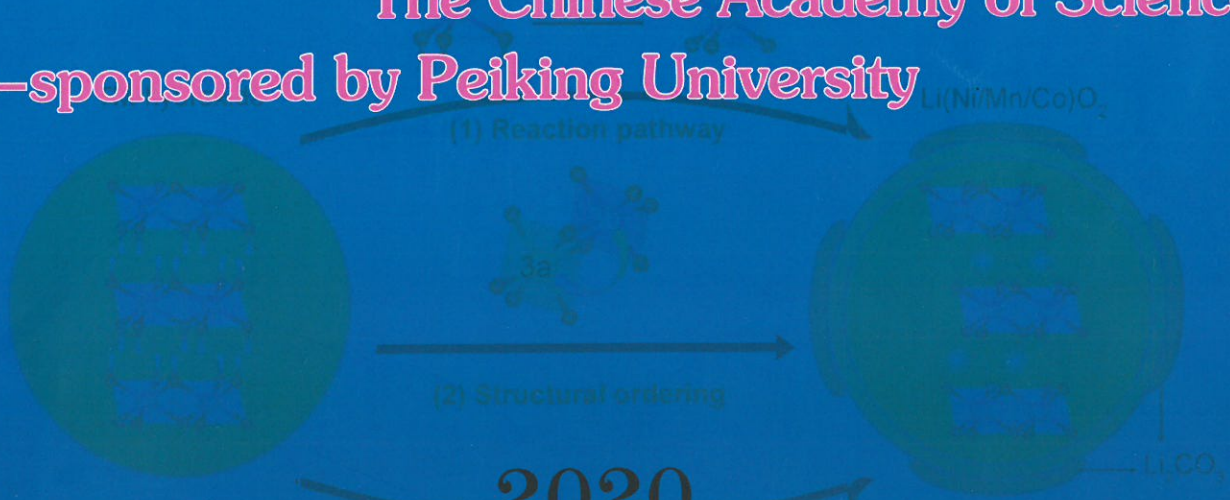

2020
Vol. 39 No. 7

Computational Study of Azide-oxirane as High-energy-density Materials

LI Bu-Tong LI Lu-Lin
YANG Chuan

Chinese J. Struct. Chem., 39, 1261(2020)

A series of azide oxirane were designed and studied at the CCSD(T)/cc-PVDZ//MP2/cc-PVDZ level. Both of the thermal stability and detonation characters are explored. Based on our calculations, all of the derivatives have enough stability to be synthesized in the further and excellent detonation characters to be regarded as the potential high-energy-density compounds.

Are the Nitro- and Amino-substituted Piperidine High-energy-density Compounds?

LI Bu-Tong LI Lu-Lin
ZHOU Quan-Bao

Chinese J. Struct. Chem., 39, 1266(2020)

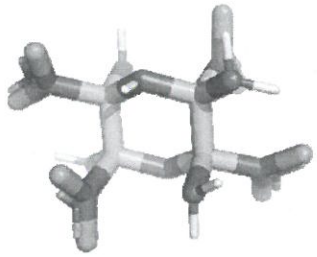

Six amino- and nitro-double substituting derivatives of piperidine were designed and calculated by using density functional theory. From our calculations, the molecule ***δ*** is screened out to be the best candidate of high-energy-density compound. All molecules have enough thermal stability to synthesize in future.

Synthesis, Crystal Structure and Biological Activity of Dimethyl 1-Methyl-1,4-dihydro-quinoline-3,4-dicarboxl ate and Tetramethyl Pyrrolo[1,2-a]quinoline-2,3,4,5-tetracarboxylate

XU Xue-Mei
LUO Zai-Gang
HAN Xin-Xin
LIU Qian-Nan
LI Rui

Chinese J. Struct. Chem., 39, 1271(2020)

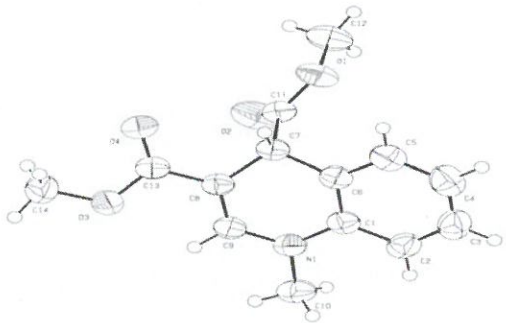

The skeleton of 1,4-dihydroquinoline **3** is noncoplanar, while pyrrolo[1,2-a]-quinoline **4** owns a coplanar frame structure. One-dimensional interaction model of compound **4** was formed by one kind of π-π interactions between the two adjacent molecules at upper and lower levels. The inhibition to the strand transfer process of HIV-1 integrase of the title compounds was also evaluated.

Isolation, Crystal Structure and Cytotoxic Activity of Natural Maistemonine and Comparison with the Synthetic Compound

WU Yi
YE Qing-Mei
QIN Shu-Qin
JIANG Ren-Wang

Chinese J. Struct. Chem., 39, 1277(2020)

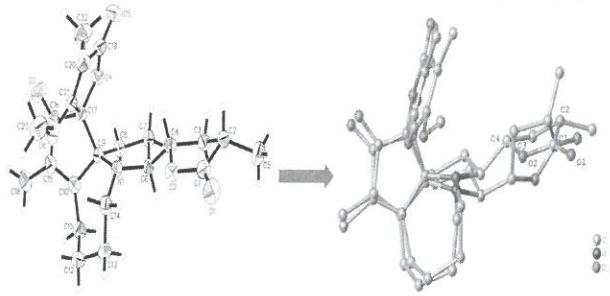

Natural maistemonine Overlay with synthetic maistemonine

The title compound maistemonine (**1**) was isolated from the 95% ethanol extractof the roots of *Stemona tuberosa*, and its structure was determined by single-crystal X-ray diffraction analysis. Compound **1** shows mild cytotoxic activity against the prostate cancer cells LNCaP and PC3 cells. The lactone ring E from the natural and synthetic **1** are almost perpendicular to each other when overlapping the remaining parts of the molecule.

Isolation, Crystal Structure and Cytotoxic Activity of Natural Maistemonine and Comparison with the Synthetic Compound①

WU Yi[a, c②] YE Qing-Mei[b, c②]
QIN Shu-Qin[c] JIANG Ren-Wang[c③]

[a] (*Zhongshan Torch Polytechnic, Zhongshan* 528436, *China*)

[b] (*Department of Pharmacy, Hainan General Hospital, Haikou* 570311, *China*)

[c] (*Guangdong Province Key Laboratory of Pharmacodynamic Constituents of Traditional Chinese Medicine and New Drugs Research, Chinese Medicine Modernization and Innovative Drug Development of Chinese Ministry of Education, Jinan University, Guangzhou* 510632, *China*)

ABSTRACT The title compound maistemonine (**1**) was isolated from the total alkaloid fraction of the 95% ethanol extract of the roots of *Stemona japonica*, followed by preparative HPLC and recrystallization from a mixture of *n*-hexane and ethyl acetate. The crystal structure of **1**, $C_{23}H_{29}NO_6$, was determined by single-crystal X-ray diffraction analysis. The crystal belongs to orthorhombic system, space group $P2_12_12_1$ with a = 8.5698(6), b = 14.0460(11), c = 17.8815(17) Å, V = 2152.4(3) Å^3, Z = 4, M_r = 415.47, D_c = 1.282 g/cm^3, λ = 0.71079 Å, μ = 0.092 cm^{-1}, F(000) = 888, S = 0.995, R = 0.0535 and wR = 0.1067. A total of 5136 unique reflections were collected, of which 3523 were observed ($I > 2\sigma(I)$). The absolute configuration of **1** could be assigned by referring to the conserved configuration of the methyl groups at C(2). Compound **1** shows mild cytotoxic activity against the prostate cancer cells LNCaP and PC3 with the IC_{50} values of 29.4 ± 2.3 and 46.6 ± 3.1 μM, respectively. It is noteworthy that the natural maistemonine (**1**) is different from the synthetic compound which was a racemic with the triclinic space group $P\bar{1}$. The lactone rings E from the natural and synthetic **1** are almost perpendicular to each other when overlapping the remaining parts of the molecules.

Keywords: maistemonine, isolation, crystal structure, cytotoxic, comparison, synthesis;
DOI: 10.14102/j.cnki.0254–5861.2011–2698

1 INTRODUCTION

Radix Stemonae derived from the roots of *Stemona tuberosa*, *S. japonica* and *S. sessilifolia* (Stemonaceae family) are often used as an antitussive Traditional Chinese Medicine to treat respiratory disorders[1]. The alkaloids possessing the nucleus of pyrrolo-azepine are the major components responsible for the antitussive activity[2, 3].

Maistemonine had ever been isolated from *Stemona pierrei*[4], *S. sessilifolia*[5] and *S. japonica*[6]. This alkaloid was found to show significant antitussive activity in a citric acid-induced guinea pig cough model following peripheral administration[5]. Quantitative determination of maistemonine was achieved by high-performance liquid chromatography coupled with diode array and evaporative light scattering detectors[7]. Due to the intriguing structure and pronounced antitussive activity, total synthesis of (±)-maistemonine was reported[8]. However, the crystal structure of natural maistemonine has not been reported yet.

Our group has been engaged in *Stemona* alkaloids for many years[9-13]. A series of alkaloids were identified from *S. tuberosa*, and some of them were found to show antitussive activities[14, 15]. During our further systematic investigation of alkaloids from *Stemona* genus, the chemical constituents of *S. japonica* were studied. Maistemonine (**1**, Scheme 1) was isolated and crystallized in a mixture solution of *n*-hexane and

Received 11 December 2019; accepted 5 March 2020 (**CCDC 1970444**)

① This work was supported by Guangdong Key Scientific Project (2013A022100029) and Guangdong Characteristic Innovation Projects of Universities (2018GKTSCX055)

② Wu Yi and Ye Qing-Mei contribute equally to this work

③ Corresponding author. E-mail: trwjiang@jnu.edu.cn

ethyl acetate. **1** was reported to show antitussive activity[5] and chemically synthesized[8]. Compound **1** has five chiral centers (C(2), C(4), C(6), C(9) and C(17)), and a precise understanding of their three-dimensional structures would be important for understanding the bioactivities. We report herein the isolation, crystal structure and cytotoxic activity of compound **1** and a detailed comparison with the synthetic compound.

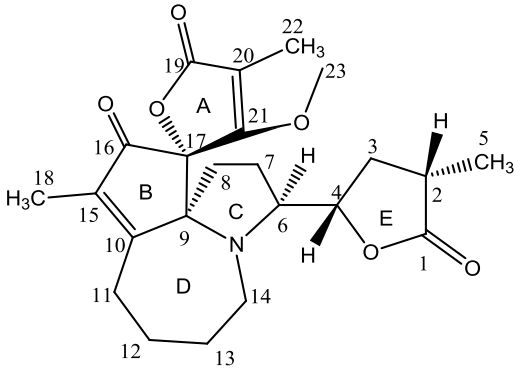

1

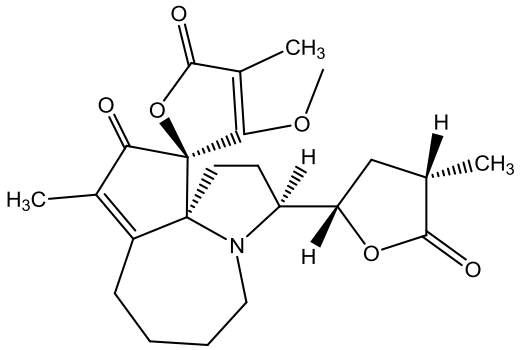

2

Scheme 1. Structures of maistemonine (1) and isomaistemonine (2)

2 EXPERIMENTAL

2. 1 Materials and instrumentations

Melting points were determined using a Fisher scientific and uncorrected. The UV spectra were obtained on a Beckman Du650 spectrophotometer in MeOH. IR spectra were recorded on a Nicolet impact 420 FT-IR spectrometer. The NMR spectra were obtained on a Bruker 400 spectrometer with chemical shift reported in δ (ppm) using TMS as the internal stand. ESIMS was recorded on a Finnigan MAT TSQ 7000 instrument. X-ray diffraction of compound **1** was conducted on a Bruker SMART1000 CCD diffractometer.

2. 2 Plant material

Roots of *Stemona japonica* were collected in Yunnan province, and were identified by Prof. Guangzhou Zhou in College of Pharmacy, Jinan University. A voucher specimen (SJ-2004) is deposited in College of Pharmacy, Jinan University.

2. 3 Extraction and preparation of maistemonine

A dry ground herbal sample of the roots *S. japonica* (1.0 kg) was percolated with 95% EtOH at room temperature for three days, and then the solution was filtered and concentrated under reduced pressure to afford a residue (86 g). The residue was acidified with 500 mL of 4% HCl solution, and then extracted with Et_2O (400 mL × 3). The Et_2O layer was evaporated to give a crude non-alkaloid extract (6 g). The pH value of the water layer was adjusted to 9.0 with 35% NH_4OH, and extracted with Et_2O to afford the total alkaloids (4.5 g). The total alkaloids (4.0 g) were subjected to preparative HPLC eluted by gradient H2O-CH3CN containing 0.1% Et3N. The peak at *Rt* = 15.7 min was collected and condensed under vacuo to afford maistemonine (**1**, 18 mg). Finally, the maistemonine was re-crystallized from a mixture of *n*-hexane-ethyl acetate (3:1) to afford colorless crystals.

Compound **1**: $C_{23}H_{29}NO_6$, m. p.: 204～205 ℃, UV (MeOH) λ_{max} 260 nm; IR (KBr) ν_{max} 1710, 1758 cm^{-1}. ESI-MS 416.2 $[M+H]^+$, 317.3 $[M+H-C_5H_7O_2]^+$.

2. 4 X-ray structure determination

The crystals suitable for X-ray structure determination were obtained by slow evaporation of *n*-hexane and ethyl acetate mixture (3:1) at room temperature. A colorless prism-like crystal of the title compound with dimensions of 0.15mm × 0.12mm × 0.10mm was selected and mounted on a thin glass fiber. Intensity data were collected at room temperature (292(2) K) on a Smart1000 CCD diffractometer using Mo$K\alpha$ radiation λ = 0.71079 Å. The data frames with a maximum 2θ value of ~55.8° were processed using the program SAINT. The data were corrected for absorption and beam corrections based on the multi-scan technique as implemented in SADABS.

A total of 5136 reflections were collected in the range of $1.8 \leqslant \theta \leqslant 27.9°$ (index ranges: $-10 \leqslant h \leqslant 11$, $-14 \leqslant k \leqslant 18$, $-23 \leqslant l \leqslant 23$) by using an ω scan mode, of which 3523 independent reflections (R_{int} = 0.061) with $I > 2\sigma(I)$ were considered as observed and used in the succeeding refinements. The structure was solved by direct methods with

SHELXS-2014 and expanded by using Fourier difference techniques. The non-hydrogen atoms were refined anisotropically, and the hydrogen atoms were added according to theoretical models. The structure was refined by full-matrix least-squares techniques on F^2 with SHELXL-2014. The final refinement gave R = 0.0535, wR = 0.1067 ($I > 2\sigma(I)$), $w = 1/[\sigma^2(F_o^2) + (0.0558P)^2 + 0.0000P]$, where $P = (F_o^2 + 2F_c^2)/3$. $(\Delta/\sigma)_{max}$ = 0.000, S = 0.995, $(\Delta\rho)_{max}$ = 0.156 and $(\Delta\rho)_{min}$ = –0.176 e/Å^3.

2. 5 Cytotoxicity assay

The MTT assay was done according to the procedures described previously[16] with cisplatin serving as the positive control. Briefly, the prostate cancer cells were plated into 96-well plates at a density of 3 × 10^3 cells per well for androgen independent cells DU145 and 5 × 10^3 cells per well for androgen dependent cell PC3 cells. After 48 h of exposure, staining with 3-(4,5-dimethyl-2-thiazolyl)-2,5-diphenyl-2-H-tetrazolium bromide (MTT) was performed. The IC_{50} values were calculated based on the absorbance at 570 nm which was measured on a multiplate reader.

Table 1. Selected Bond Lengths (Å) and Bond Angles (°)

Bond	Dist.	Bond	Dist.
O(1)–C(1)	1.199(3)	O(5)–C(19)	1.208(4)
O(2)–C(1)	1.365(3)	O(6)–C(21)	1.334(3)
O(2)–C(4)	1.453(3)	O(6)–C(23)	1.434(4)
O(3)–C(16)	1.218(4)	N(1)–C(14)	1.455(3)
O(4)–C(19)	1.374(4)	N(1)–C(6)	1.460(3)
O(4)–C(17)	1.430(3)	N(1)–C(9)	1.466(3)
Angle	(°)	Angle	(°)
C(14)–N(1)–C(6)	118.2(2)	N(1)–C(9)–C(17)	113.2(2)
C(14)–N(1–C(9)	120.6(2)	C(10)–C(9)–C(17)	101.8(2)
C(6)–N(1)–C(9)	111.8(2)	C(8)–C(9)–C(17)	110.9(2)
O(2)–C(4)–C(6)	111.4(2)	C(15)–C(10)–C(11)	126.2(3)
O(2)–C(4)–C(3)	103.6(2)	C(15)–C(10)–C(9)	112.3(3)
C(6)–C(4)–C(3)	114.3(2)	C(11)–C(10)–C(9)	121.1(3)
N(1)–C(6)–C(4)	113.8(2)	O(4)–C(17)–C(21)	103.4(2)
N(1)–C(6)–C(7)	104.1(2)	O(4)–C(17)–C(16)	112.5(2)
C(4)–C(6)–C(7)	108.4(2)	C(21)–C(17)–C(16)	109.8(2)
N(1)–C(9)–C(10)	117.7(2)	O(4)–C(17)–C(9)	112.7(2)
N(1)–C(9)–C(8)	104.3(2)	C(21)–C(17)–C(9)	115.6(2)
C(10)–C(9)–C(8)	109.0(2)	C(16)–C(17)–C(9)	103.1(2)

Table 2. Intermolecular C–H ··O Interaction[17] Lengths (Å) and Angles (°)

D–H ··A	d(D–H)	d(H ··A)	d(D ··A)	∠DHA
C(14)–H(14A) ··O(6)	0.97	2.36	3.147(4)	138
C(14)–H(14B) ··O(2)	0.97	2.36	3.070(4)	130
C(3)–H(3A) ··O(5)[a]	0.97	2.66	3.581(3)	159
C(3)–H(3B) ··O(3)[b]	0.97	2.73	3.494(4)	136
C(22)–H(22A) ··O(2)[c]	0.96	2.81	3.467(2)	126
C(18)–H(18A) ··O(1)[d]	0.96	2.72	3.430(3)	131

Symmetry codes: (a) x – 1, y, z; (b) 1.5 – x, 1 – y, z – 0.5; (c) x + 1, y, z; (d) 1 – x, y + 0.5, 1.5 – z

3 RESULTS AND DISCUSSION

Compound **1** was obtained from the total alkaloid fraction of the 95% ethanol extract followed by preparative HPLC (detection at 260 nm, Fig. 1). The peak at 15.7 min was collected, concentrated under reduced pressure and recrystallized as colorless prism-like crystals. High resolution ESIMS analysis of **1** showed a quasi-molecular ion peak at $[M+H]^+$ 416.2060, corresponding to a molecular formula $C_{23}H_{30}NO_6$ (calculated 416.2068). Its IR spectrum (KBr) showed the presence of two γ-lactone rings (1710, 1758 cm^{-1}). The ESI mass spectrum showed $[M+H]^+$ at m/z 416.2 and the base peak at m/z 317.3 $[M+H\text{-}C_5H_7O_2]^+$, indicating the presence of typical β-methyl-γ-lactone ring annexed to C(3) of the azepine ring.

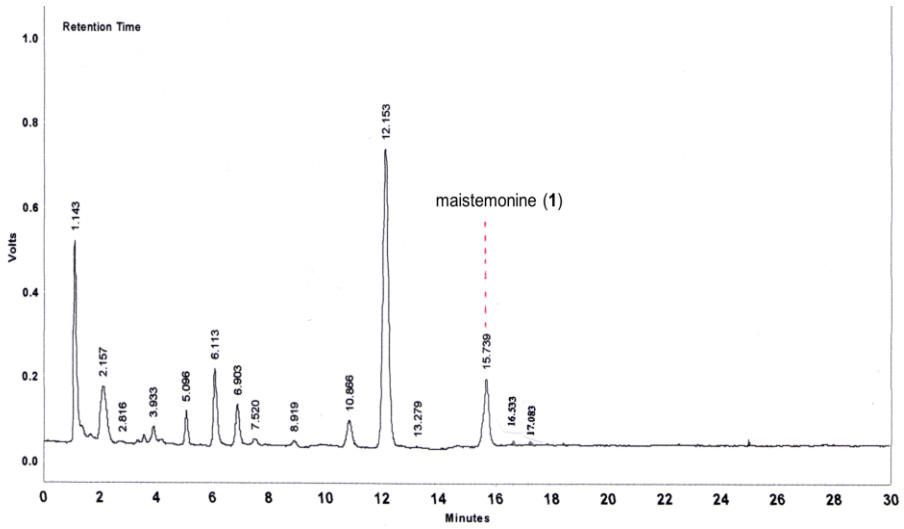

Fig. 1. HPLC chromatogram of total alkaloid of *S. japonica*, showing the presence of maistemonine (1) and the highest peak protostemonine. Column: C 18 column (Alltech, 250 × 4.6 cm, 5 μm); mobile phase: (A) H_2O-(B) CH_3CN containing 0.1% Et_3N, gradient: 0～10 min isocratic 40% B, 10～12 min linear 40% to 50% of B; 12～28 min isocratic 50% B and 28～30 min linear 50% to 40% of B; flow rate: 1.0 mL/min; detection: 260 nm

The ^{1}H-NMR spectrum of compound **1** showed a doublet (*d*, J = 7.2 Hz, 3H) at δ_H 1.24 for the C(5) methyl group, two singlets (*s*, 3H each) at δ_H 2.06, corresponding to the two methyl groups on a double bond C(18) and C(22), a singlet at δ_H 4.00 (*s*, 3H, H-23) attributed to a methoxy group and a low-field proton attached to carbon atoms bearing an oxygen function at δ_H at 3.85 (*ddd*, J = 6.0, 7.8, 11.2 Hz, 1H, H-4), a methine and two geminal protons attached to carbon atoms bearing a nitrogen function at δ_H 3.59 (*m*, 1H, H-6), δ_H 3.38 (*m*, 1H, H-14β) and δ_H 2.90 (*m*, 1H, H-14α). The ^{13}C-NMR spectrum showed a saturated lactone ring (δ_C 179.5, 34.2, 34.1, 84.7), an α,β-unsaturated lactone ring (δ_C 175.2, 97.0, 172.0, 91.5) and an α,β-unsaturated ketone ring (δ_C 196.8, 135.0, 175.1, 79.6, 91.5). These spectroscopic data are reminiscent of the protostemonine-type alkaloids bearing an α-methyl-γ-lactone ring annexed to C-3[3].

The crystal belongs to orthorhombic system with space group $P2_12_12_1$. Selected bond lengths and bond angles of compound **1** are given in Table 1. Fig. 2 shows the molecular structure of the title compound, and Fig. 3 depicts the packing diagram. X-ray analysis confirmed the presence of an α,β-unsaturated lactone ring (A), a α,β-unsaturated ketone ring (B), a tetrahydropyrrole ring (C), a seven-membered hetercyclic ring (D), and a saturated lactone ring (E).

Ring A is planar with the mean derivation of 0.0123(4) Å. The five-membered rings B, C and E all adopt envelope conformations with C(17), C(7) and C(3) displaced by –0.3583(2), 0.5325(3) and –0.5535(2) Å from the mean planes of the remaining four atoms in each ring, respectively. The seven-membered heterocyclic ring D adopts a chair conformation with N(1), C(9) and C(12) deviating by –1.0236, –0.8973 and 0.6996 Å from the least-squares plane (C(10), C(11), C(13) and C(14)), respectively. Rings A and B are connected through a spiro-atom C(17) and are roughly perpendicular to each other with a dihedral angle 88.1°.

The relative configurations of the chiral centers C(2), C(4), C(6), C(9) and C(17) were established to be *rel*-(*S*, *S*, *S*, *S* and *S*), respectively, and both the C(10)–C(15) and C(20–C(21) double bonds are *E*-configurations. Compound **1** is an isomer of isomaistemonine (**2**) at C(17), which can be synthesized from **1** through a retro-Mannich process[8]. It is here named maistemonine. Due to the absence of heavy atom in the molecule, the final refinement resulted in a non-significant Flack parameter; however, considering the conserved α-orientated methyl group at C(2) in Stemona alkaloids[3, 12], the absolute configuration of compound **1** could be assigned as shown in Fig. 2.

No typical intermolecular hydrogen bonds were found in the crystal structure. In solid state, intermolecular weak C–H···O interactions[17] (Table 2) linked the molecules into a three-dimensional assembly (Fig. 3).

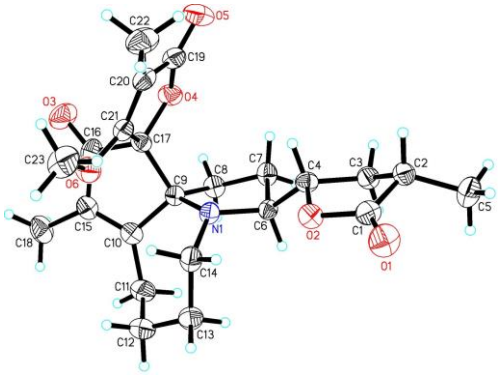

Fig. 2. Molecular structure of 1, showing 30% probability displacement ellipsoids and the atom-numbering scheme

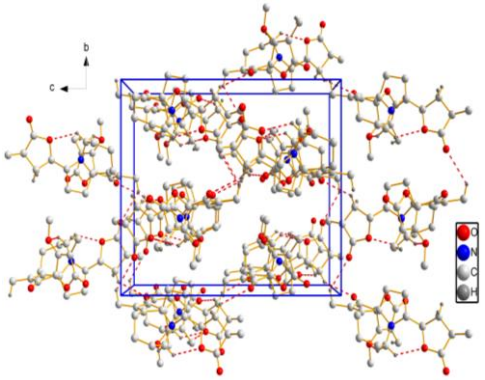

Fig. 3. A packing diagram for compound 1 viewed roughly down the *a*-axis. Selected hydrogen atoms highlight the scheme of hydrogen bonds

The synthesis of natural products offers a reliable way to confirm the complete structure of natural products; however, most natural products are chiral and the synthetic compounds are often racemic. For the natural alkaloid **1**, the absence of h00, 0k0 and 00l reflections when *h*, *k*, and *l* are odd numbers clearly indicated space group $P2_12_12_1$. In contrast, for the corresponding synthetic compound[8], the crystal belongs to triclinic system with space group $P\bar{1}$. Furthermore, significant conformational changes were observed in the lactone ring E (Fig. 4), which were evidenced by the torsion angles of N(1)–C(6)–C(4)–O(2) (63.7°) and N(1)–C(6)–C(4)–C(3) (–179.2°) for the natural **1**, in contrast to the corresponding angles from the synthetic compound (–173.5° and –54.8°, respectively). When overlapping A, B, C and D rings of the natural and synthetic compound, rings E from the two compounds are almost perpendicular to each other (Fig. 4).

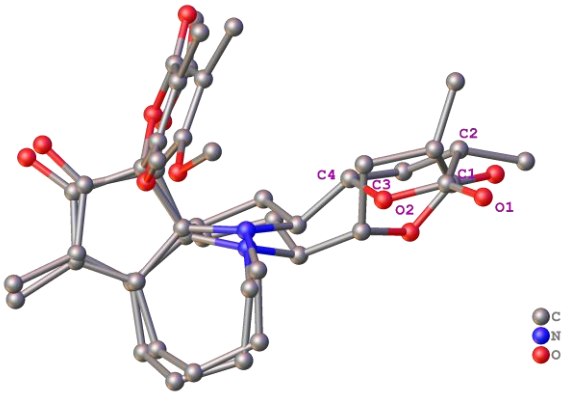

Fig. 4. Overlap of the natural 1 (with atom labels) and the synthetic compound with Olex 2 software. When overlapping A, B, C and D rings of the natural and synthetic compound, rings E from the two compounds are almost perpendicular to each other. For clarity, only ring E of the natural 1 was labeled

Besides the antitussive activity, the cytotoxicity[4] and anti-insect properties[18] of Stemona alkaloids were often investigated. The antitussive activity of **1** have been reported before[5]. The cytotoxic property of **1** was evaluated herein which was studied using a standard MTT procedure[16]. Compound **1** shows mild cytotoxic activity against the prostate cancer cells LNCaP (an androgen dependent prostate cancer cell) and PC3 (an androgen independent prostate cancer cell) with the IC_{50} values of 29.4 ± 2.3 and 46.6 ± 3.1 μM, respectively, which are around three times weaker than the positive control cisplatin (10.1 ± 1.3 for LNCaP cells and 15.4 ± 1.6 μM for PC3 cells).

In summary, we report herein the crystal structure of maistemonine (**1**), which is a natural product isolated from the roots of *Stemona japonica*. We found that the natural maistemonine is completely different from the corresponding synthetic compound because the former is chiral while the latter is racemic. Furthermore, the E-rings of the natural product and the synthetic compound showed completely different orientation, suggesting that artificial synthesis is difficult to replace the natural sources. It is noteworthy that the cytotoxic activity is reported here for the first time.

CONTRIBUTION OF AUTHORS

We declare that this work was done by the authors named in this article. Jiang Ren-Wang designed the study and the experiments. Wu Yi performed the isolation and identification of maistemonine, Ye Qing-Mei performed the bioassay on the inhibitory activities of maistemonine on cancer cells and Qin Shu-Qin carried out the X-ray crystallographic analysis of maistemonine.

REFERENCES

(1) Pharmacopoeia commission of People's Republic of China. *The Pharmacopoeia of the People's Republic of China, Part 1*. Chemical Industry Publishing House, Beijing, China **2015**, p204.

(2) Pilli, R. A.; Rossoa, G. B.; Oliveira, M. C. The chemistry of Stemona alkaloids: an update. *Nat. Prod. Rep.* **2010**, 27, 1908–1937.

(3) Greger, H. Structural relationships, distribution and biological activities of Stemona alkaloids. *Planta Med.* **2006**, 72, 99–113.

(4) Quang, D. N.; Khamko, V. A.; Trang, N. T.; Yen, L. T. H.; Dien, P. H. Stemofurans X-Y from the roots of Stemona species from Laos. *Nat. Prod. Commun*. **2014**, 9, 1741–1742.

(5) Yang, X. Z.; Zhu, J. Y.; Tang, C. P.; Ke, C. Q.; Lin, G.; Cheng, T. Y.; Rudd, J. A.; Ye, Y. Alkaloids from roots of *Stemona sessilifolia* and their antitussive activities. *Planta Med*. **2009**, 75, 174–177.

(6) Yi, M.; Xia, X.; Wu, H. Y.; Tian, H. Y.; Huang, C.; But, P. P. H.; Shaw, P. C.; Jiang, R. W. Structures and chemotaxonomic significance of stemona alkaloids from *Stemona japonica*. *Nat. Prod. Commun*. **2015**, 10, 2097–2099.

(7) Li, S. L.; Jiang, R. W.; Hon, P. M.; Cheng, L.; Xu, H. X.; Greger, H.; But, P. P. H.; Shaw, P. C. Quality evaluation of Radix Stemonae through simultaneous quantification of bioactive alkaloids by high-performance liquid chromatography coupled with diode array and evaporative light scattering detectors. *Biomed. Chromatogr*. **2007**, 21, 1088–1094.

(8) Chen, Z. H.; Chen, Z. M.; Yang, Y. Q.; Tu, Y. Q.; Zhang, F. M. Total synthesis of (±)-maistemonine, (±)-stemonamide, and (±)-isomaistemonine. *J. Org. Chem.* **2011**, 76, 10173–10186.

(9) Jiang, R. W.; Hon, P. M.; But, P. P. H.; Chung, H. S.; Lin, G.; Ye, W. C.; Mak, T. C. W. Isolation and stereochemistry of two new alkaloids from *Stemona tuberose* Lour. *Tetrahedron* **2002**, 58, 6705–6712.

(10) Jiang, R. W.; Hon, P. M.; Xu, Y. T.; Chan, Y. M.; Xu, H. X.; Shaw, P. C.; But, P. P. H. Isolation and chemotaxonomic significance of tuberostemospironine-type alkaloids from Stemona tuberosa. *Phytochemistry* **2006**, 67, 52–57.

(11) Wu, Y.; Ye, Q. M.; Liu, J.; Xu, W.; Zhu, Z. R.; Jiang, R. W. Isolation, crystal structure and antitussive activity of 9S,9aS-neotuberostemonine. *Chin. J. Struct. Chem.* **2018**, 37, 571–576.

(12) Jiang, R. W.; Hon, P. M.; Zhou, Y.; Chan, Y. M.; Xu, Y. T.; Xu, H. X.; Greger, H.; Shaw, P. C.; But, P. P. H. Alkaloids and chemical diversity of *Stemona tuberosa*. *J. Nat. Prod*. **2006**, 69, 749–754.

(13) Jiang, R. W.; Ye, W. C.; Shaw, P. C.; But, P. P. H.; Mak, T. C. W. Absolute configuration of neostenine. *J. Mol. Struct*. **2010**, 966, 18–22.

(14) Xu, Y. T.; Hon, P. M.; Jiang, R. W.; Cheng, L.; Li, S. H.; Chan, Y. P.; Xu, H. X.; Shaw, P. C.; But, P. P. H. Antitussive effects of *Stemona tuberosa* with different chemical profiles. *J. Ethnopharmacol.* **2006**, 108, 46–53.

(15) Xu, Y. T.; Shaw, P. C.; Jiang, R. W.; Hon, P. M.; Chan, Y. M.; But, P. P. H. Antitussive and central respiratory depressant effects of *Stemona tuberosa*. *J. Ethnopharmacol*. **2010**, 128, 679–684.

(16) Mosmann, T. Rapid colorimetric assay for cellular growth and survival: application to proliferation and cytotoxicity assays. *Journal of Immunological Methods* **1983**, 65, 55–63.

(17) Desiraju, G. R.; Steiner, T. *The Weak Hydrogen Bond in Structural Chemistry and Biology*. Oxford University Press, New York **1999**.

(18) Brem, B.; Seger, C.; Pacher, T.; Hofer, O.; Vajrodaya, S.; Greger, H. Feeding dterrence and cntact toxicity of stemona alkaloids, a source of potent natural insecticides. *J. Agric. Food Chem.* **2002**, 50, 6383–6388.